

External Diamagnetic and Paramagnetic Passive Shimming of the Human Brain

K. M. Koch¹, P. B. Brown¹, D. L. Rothman¹, and R. A. de Graaf¹

¹Magnetic Resonance Research Center, Yale University, New Haven, CT, United States

Introduction Room-temperature (RT) spherical harmonic shimming technology cannot adequately compensate global *in vivo* subject-specific B_0 inhomogeneity within the human brain. Furthermore, improvements in existing RT shim capabilities are limited by available bore space and the Biot-Savart law. Subject-targeted passive shims can however enable further homogenization.[1][2][3] Here, we present subject-specific passive shimming of residual higher-order inhomogeneity in the human brain using a combination of highly diamagnetic (bismuth, $\chi = -166$ ppm) and paramagnetic (niobium, $\chi = +225$ ppm) materials. Unlike previous local shimming approaches on the human brain [2][4], the presented passive shim system does not require placement of shim hardware in the mouth of patients. This is a significant advantage when patient comfort is factored into the overall utility of the passive shim system. Compared to global RT shimming, measurable reduction of residual global B_0 inhomogeneity is demonstrated using this passive shim system.

Methods Experiments were performed at Yale University's W.F. Keck high-field magnetic resonance laboratory on a 4.0 T Bruker MedSpec system.

The current investigation was aimed to establish the utility of combined diamagnetic and paramagnetic passive shimming on the human brain through manual shim optimization. Rapid magnetostatic solutions of the fields induced by arbitrary magnetic susceptibility distributions [5][6][7] provide tremendous assistance in such manual shim optimization. Figure 1 provides a validation of the accuracy of these methods in predicting the induction fields from typical shim elements. The difference map between computed and measured induction fields from the given bismuth shim element conclusively demonstrates the accuracy of the computational protocol.

Shims were constructed to locally target residual inhomogeneity near the auditory and sinus cavities. Both bismuth and niobium metals were used to develop shim fields which selectively targeted these regions. Computational assessment and adjustment of shim geometries was scripted in Matlab and executed on a Dell precision workstation with dual 2.7 GHz processors and 3 GB of RAM. Figure 2 provides the details of the constructed shim assembly.

Results and Discussion Figure 3 demonstrates improvements in residual inhomogeneity when using passive shims in combination with available second-order RT shims. RT shim settings were determined through least-squares optimization over whole-brain ROIs. Magnetic field maps were calculated from 4 gradient-echo images acquired with different echo times of $TE = 8$ ms + [0.5, 1.5, 4.0] ms and $TR = 25$ ms. Images were collected over 64 0.5 cm slices with a 24 cm x 24 cm FOV and 96 x 96 data-matrix. Individual phase images were unwrapped through temporal extrapolation. Clear improvements were made over stand-alone RT shimming through use of the passive-shim system.

To demonstrate the impact of such improvements, gradient-echo images with $TE = 35$ ms were collected to demonstrate signal-loss reduction with the passive shim system. Echo times of at least 30 ms are typically utilized to develop BOLD contrast. Improvements in signal recovery are therefore representative of passive-shim utilized signal recovery in fMRI studies. Images were obliqued by 25 degrees to show signal recovery near both the auditory and sinus cavities in the same slice. Figure 4 presents these results, where significant reduction of signal loss is demonstrated through use of the passive shim system. Extensive B_1 mapping showed no significant RF interaction with the shim system. This is likely due to the relatively low electrical conductivities of bismuth and niobium, along with the use of discretized shim element distributions.

These results show that external combined diamagnetic and paramagnetic passive shimming can significantly improve upon the global human brain homogenization capabilities of existing shim technology. Further work will investigate more rigorous optimization strategies in both the construction of shims and patient-specific placement/design. Combined diamagnetic and paramagnetic passive shimming of the human brain may be possible using our previously published linear optimization method. [3] However, implementation of this algorithm on the human will likely require more complicated shim grids (i.e multiple-surfaces or three-dimensional) than those previously utilized in global shimming of the mouse brain. *NIH Grant Support: R21 CA118503 and R01 EB00473*

- [1] A. Jesmanowicz et al, USPTO 6,294,972 (2001) [5] JP Marques, R. Bowtell, *CMR B*, 25B, 65-78 (2005)
 [2] J. Wilson et al, *MRM*, 48, 906-914 (2002) [6] R. Salomir et al, *CMR B*, 19B, 26-34, (2003)
 [3] Koch et al, *JMR*, 182, 66-74 (2006) [7] KM Koch et al, *Phys. Med. Biol.* (2006), in press
 [4] Hsu et al, *MRM*, 53, 243-248 (2005)

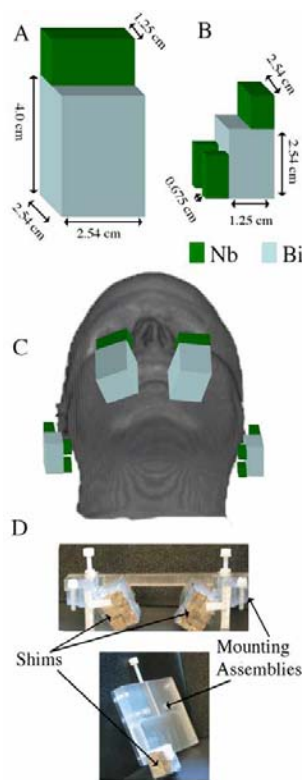


Figure 2: Constructions of A) sinus shims, B) auditory shims, C) and positioning relative to head, and D) photographs of shim and mounting assemblies

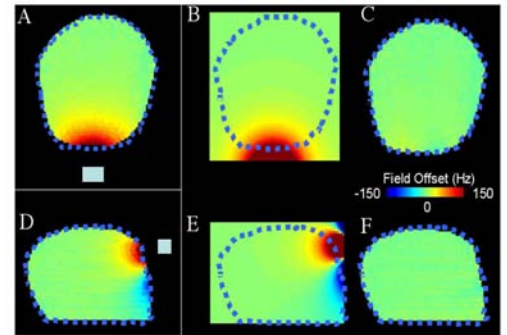


Figure 1: Measured (A,D), computed (B,E), and difference (C,F) maps of fields induced by 2.54 x 1.12 x 0.60 cm Bi shim element in axial (A-D) and sagittal (D-F) orientations.

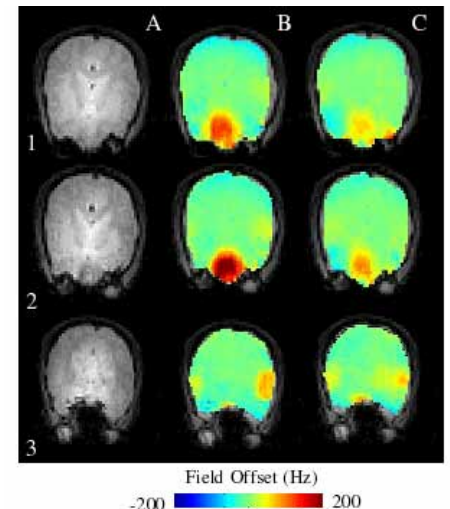


Figure 3: A) FLASH MRI images of axial slices (1-3), magnetic field maps after B) RT shim optimization, and C) RT and passive shim optimization

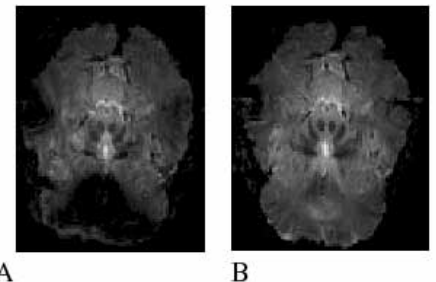


Figure 4: Oblique gradient-echo images collected with $TE = 35$ ms (representative of echo times used for BOLD contrast) A) without and B) with use of passive shim system